AJNR

An experimental arteriovenous malformation model in swine: anatomic basis and construction technique.

T F Massoud, C Ji, F Viñuela, G Guglielmi, J Robert, G R Duckwiler and Y P Gobin

An Experimental Arteriovenous Malformation Model in Swine: Anatomic Basis and Construction Technique

Tarik F. Massoud, Cheng Ji, Fernando Viñuela, Guido Guglielmi, John Robert, Gary R. Duckwiler, and Y. Pierre Gobin

Summary: We assessed the feasibility of creating an experimental arteriovenous malformation model in swine by diverting and increasing blood flow through bilateral retia mirabilia. This was achieved by surgical formation of a large right-sided carotid-jugular fistula, in combination with endovascular occlusion of several neck arteries ipsilateral to the fistula. Using this technique, 11 of 13 swine demonstrated an acute-phase angiographic simulation of an arteriovenous malformation. There was rapid circulatory diversion from the left ascending pharyngeal artery ("feeder"), across both retia ("nidus"), and fast retrograde flow into the right ascending pharyngeal and common carotid arteries ("draining vein") toward the fistula. The relevant vascular anatomy of the swine head and neck is outlined, and steps in the construction of this arteriovenous malformation model are detailed.

Index terms: Arteriovenous malformations; Fistula, arteriovenous; Interventional neuroradiology, models; Animal studies

Arteriovenous malformations (AVMs) are the most common symptomatic congenital vascular malformation of the central nervous system (1). They are said to be vascular hamartomas with an arteriovenous shunt of variable degree between feeding arteries and draining veins, resulting from a disorder of embryogenesis (2). Histologically, the site of this shunt consists of a conglomerate of abnormal vessels (the nidus) of variable diameter and wall thickness. Depending on the degree of destruction of the embryonal vascular plexus, the nidus may be predominantly plexiform or fistulous or of mixed variety. A characteristic feature is the absence of capillaries.

Despite significant advances in the last decade, the basic study and clinical management of cerebral AVMs remain one of the most diffi-cult areas of vascular neurosurgery and neuroendovascular therapy. The difficulties in studying the many unresolved problems concerning the behavior of AVMs (with and without treatment) in part are caused by the absence of naturally occurring animal models. Models are necessary to achieve reproducibility—an essential component of scientific experimentation. Thus, in vitro models have been created using plastic mesh and tubing to gain experience with the procedure of transcatheter embolization (3, 4). Computer mathematical modeling also has been used as a theoretical means to predict hemodynamic changes during embolization (5). Previously reported in vivo models in rats (6, 7), cats (8), and monkeys (9) were created mainly to investigate pathophysiologic derangements accompanying AVMs such as cerebral steal and perfusion pressure breakthrough, but none of these models possess an AVM nidus. The carotid rete mirabile of swine (a fine network of vessels, with connections across the midline, situated at the termination of both ascending pharyngeal arteries as they perforate the skull base) has some morphologic similarities to an AVM nidus (10) but lacks its inherent arteriovenous shunting. Hence, an experimental porcine model of an AVM has been developed previously by iatrogenic traumatic shunting from the rete into the surrounding cavernous sinus (11). Drawbacks of this model, however, include (a) that it requires the relatively invasive insertion of a long spinal needle through the animal's orbit, with consequent postprocedural orbital hemor-

rhages and proptosis; (*b*) that it involves iatrogenic puncture/transection of the rete vessels (ie, trauma to the "nidus" of the "AVM"), and (*c*) that ensuing spontaneous thrombosis readily occurs because arteriovenous shunting is at the level of the normal rete microvessels, thus this model is essentially limited to being an acute-phase one. All these drawbacks are avoided in our present model.

We report the experimental creation of an in vivo AVM model, entailing principally the simple surgical formation of a carotid-jugular fistula in the neck of swine. In addition to possessing the prime characteristics of an AVM (rapid shunting through a nidus), this model appears to offer two major benefits that represent a significant advance in experimental in vivo modeling of these vascular malformations: simplicity of creation, and clear visualization of all components of the "AVM," including an intact nontraumatized "nidus."

Methods

All animal experimentation was conducted in accordance with policies set by the local University Chancellor's Animal Research Committee and National Institutes of Health guidelines. Thirteen Red Duroc swine were used in this preliminary feasibility study. The animals were 3 to 4 months old, weighed 30 to 40 kg, were of mixed sex, and were maintained on standard laboratory diet. After an overnight fast, each swine was premedicated with 20 mg/kg ketamine and 2 mg/kg xylazine intramuscularly. General anesthesia was maintained with mechanical ventilation and inhalation of 1% to 2% halothane after endotracheal intubation.

Baseline Angiography

Under general anesthesia, a 7F angiographic sheath was placed in the femoral artery following standard Seldinger puncture and catheterization. Via this transfemoral route, a selective left and then right common carotid arteriogram was performed using a tapered 5.5-4F Viñuela catheter (Cook, Bloomington, Ind). Six mL of iohexol 350 mg I/mL (Sanofi Winthrop Pharm, NY) were injected to outline the normal arterial (Fig 1) and venous (on delayed imaging) anatomy of the head and neck in anteroposterior and lateral views.

Endovascular Occlusion of Neck Vessels

Endovascular occlusion of three arteries in the swine's neck was necessary to maximize postoperative blood channeling from the rete to the fistula. Previous pilot investigations had demonstrated that when these arteries were left unoccluded after fistula formation, they participated in major collateral pathways that diverted most of the blood flow from the opposite side of the head and neck to the fistula, while bypassing the rete itself.

The Viñuela catheter was exchanged over a guidewire for a 7F Royal Flush guiding catheter (Cook, Bloomington, Ind). The latter was connected to a Touhy-Borst Y-connector to allow coaxial insertion of a Tracker 18 microcatheter/Seeker 14 microguidewire combination (Target Therapeutics, Fremont, Calif). A bolus intraarterial dose (3000 U) of heparin was given. With fluoroscopic and road-map visualization in the lateral radiographic plane, the right occipital artery and the muscular branch of the right ascending pharyngeal artery in turn were selectively catheterized. Both arteries were endovascularly occluded just beyond their origins by placement of simple coils (Target Therapeutics, Fremont, Calif) or more easily by endovascular monopolar electrocoagulation via the microguidewire (Fig 2). Next, the microcatheter and microguidewire were removed, and an inflatable balloon (hand tied or Goldvalve detachable balloon [size 16] [Ingenor, France]) mounted on a Tracker 18 microcatheter was introduced and navigated to the origin of the right external carotid artery. At this site, the balloon was inflated and released to obtain permanent vessel occlusion.

Surgical Fistula Formation

Carotid-jugular fistula formation is a standard and well-described surgical procedure in laboratory animals (12) but is only of historical interest in humans (13). Briefly, the right side of the neck was shaved and scrubbed with betadine solution then draped in a sterile fashion. Under sterile conditions, a 10-cm incision was made in the neck parallel to the sternocleidomastoid muscle. Self-retaining retractors were used to facilitate exposure. Reflecting the sternocleidomastoid muscle medially, a 3-cm segment of the external jugular vein, free of tributaries, was dissected, isolated, and cleaned of adventitia. Next, a 3-cm adjacent segment of the common carotid artery also was dissected, isolated, and cleaned of adventitia. Vasoconstriction caused by handling of the artery and vein was relieved by topical application of papaverine hydrochloride. Four small vascular clamps then were placed at each end of the isolated common carotid artery and external jugular vein segments to achieve temporary occlusion during fistula creation. Using a microscalpel or microscissors, opposing 2-cm long elliptical arteriotomy and venotomy were fashioned. The posterior margins of these were approximated and anastomosed using a continuous 7–0 prolene suture, starting from one corner to the other. After washing the vessel lumens with heparinized saline, the anterior margins of the arteriotomy and venotomy were anastomosed similarly to form a side-to-side arteriovenous fistula. The vascular clamps subsequently were removed to reveal marked dilatation and pulsation of the external jugular vein caused by the presence of arterialized blood. The right common carotid artery caudad to the fistula was ligated (or balloon occluded) in all models. Subcutaneous tissues and skin were sutured in layers. During the procedure, the
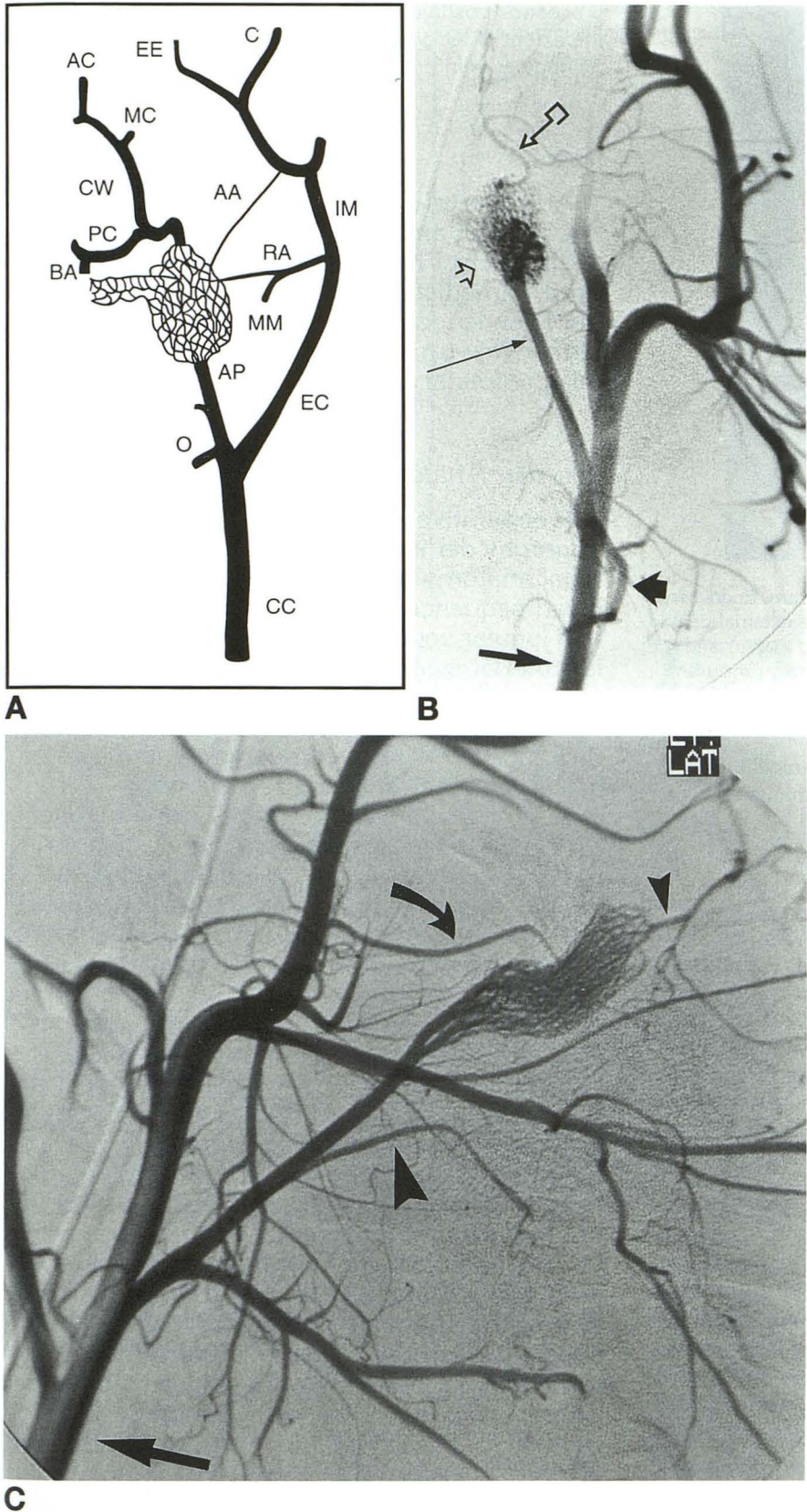
A

B

Fig 1. Normal arterial anatomy of the swine head.

A, Schematic diagram in the frontal plane (modified from Daniel et al [21]).

B, Frontal view of left common carotid arteriogram.

C, Lateral view of left common carotid arteriogram.

Note.—CC indicates common carotid artery (*long thick arrow*); EC, external carotid artery; IM, internal maxillary artery; MM, middle meningeal artery supplying the ramus anastomoticus; RA, ramus anastomoticus (*curved solid arrow*); AA, arteria anastomotica; AP, ascending pharyngeal artery (*long thin arrow*); O, occipital artery (*short thick arrow*); BA, basilar artery; PC, posterior cerebral artery; MC, middle cerebral artery; AC, anterior cerebral artery; C, ciliary artery; EE, external ethmoidal artery; *large arrowhead*, muscular branch of ascending pharyngeal artery; *open straight arrow*, rete mirabile; *small arrowhead*, internal carotid artery; and *square-ended arrow*, circle of Willis (CW).
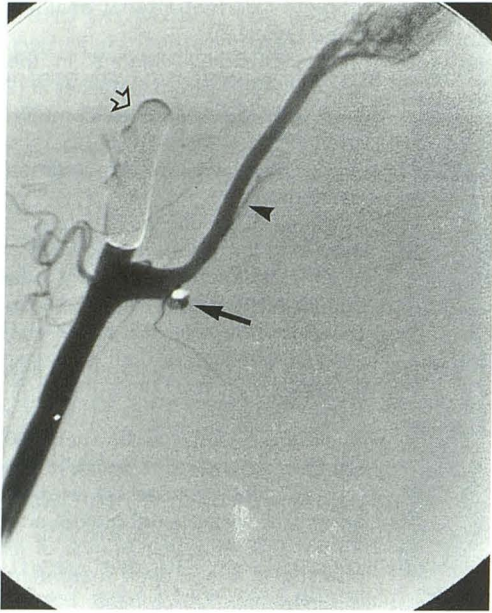

C

Fig 2. Lateral right common carotid arteriogram. Endovascularly placed permanent balloon is inflated in the external carotid artery (*open arrow*). The occipital artery (*solid arrow*) and the muscular branch of the ascending pharyngeal artery (*arrowhead*) have been occluded by endovascular electrocoagulation.

swine received 0.9 to 1.2×10^6 units of penicillin G intramuscularly. No systemic heparin was administered after surgery.

Postoperative Angiography

Immediate postoperative angiography was performed in all swine by selective injection of the left common carotid artery and ascending pharyngeal artery to demonstrate blood flow diversion through both retia. Standard (3 frames/s) and rapid-sequence cine (30 frames/s) digital subtraction images were obtained in anteroposterior, and in anteroposterior with 45° tilted craniocaudal angulation, using a GE Advantx DX HiLine digital imaging system.

Further angiographic demonstration of blood diversion from the rete to the fistula was obtained after superselective catheterization of the two minor branches from the external carotid artery that also supply the rete, the ramus anastomoticus, and the arteria anastomotica (vide infra). For these two vessels, a Tracker 10 microcatheter (Target Therapeutics, Fremont, Calif) was used. Fluoroscopic and road-mapping guidance was performed best in the anteroposterior or lateral projections for the ramus anastomoticus, and the anteroposterior projection for the arteria anastomotica. As for ascending pharyngeal artery injections, angiographic sequences were obtained best in anteroposterior or craniocaudal projections. Both retia usually were superimposed on the lateral projection, precluding adequate visualization.

After ascending pharyngeal artery injection with a large volume of contrast medium (10 mL), delayed (more than

5 seconds postinjection) images were obtained to outline the extent of retrograde and orthograde filling of the external jugular vein.

Results

All swine tolerated the general anesthesia and the surgical and endovascular procedures with no ill effects. The constructed AVM models were used immediately for training in endovascular therapeutic techniques. Consequently, no long-term follow-up investigations were conducted in this preliminary study.

Vascular Anatomy

Preoperative selective common carotid arteriography demonstrated the relevant normal arterial anatomy of the swine head and neck. Delayed sequences also revealed the intracranial and jugular venous drainage. The vertebrobasilar arterial system was not investigated in this study. In brief, the common carotid artery in the swine (which is approximately 5 mm in size) divided into external carotid artery and ascending pharyngeal artery. The latter was 2 to 2.5 mm in size and was the main artery supplying the brain (the posterior contribution to the circle of Willis is relatively minor in the swine), dividing into a compact plexus of intertwining micro-arteries (the rete mirabile) before reconstituting as a relatively short internal carotid artery, which supplied the circle of Willis. Both retia mirabilia anastomosed across the midline and were surrounded by the cavernous sinus. The occipital artery (originating at the base of the ascending pharyngeal artery) and the muscular branch of the ascending pharyngeal artery (originating half way up the ascending pharyngeal artery) anastomosed freely across the midline with the analogous contralateral arteries and with branches of the vertebral arteries. Two minor branches (less than 1 mm in size), both from the external carotid system, also supplied each rete. One was the ramus anastomoticus (a branch of the middle meningeal artery), and the other was the arteria anastomotica (a branch of the external ophthalmic artery). Venous drainage from the superior sagittal and both transverse sinuses was mostly to the spinal epidural venous plexus, with minor filling of both internal jugular veins and the cavernous sinus. The external jugular
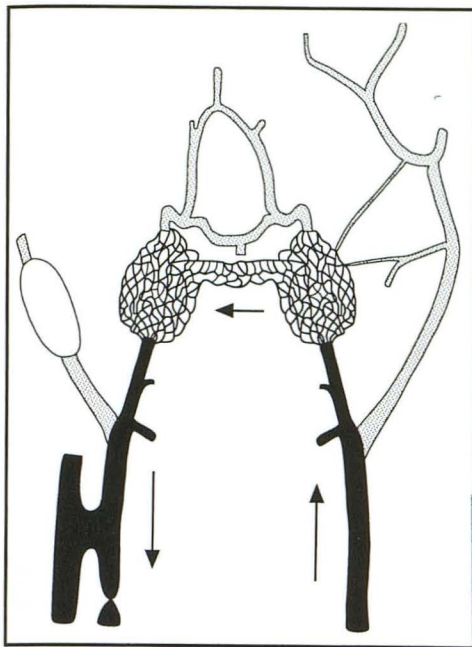
Fig 3. Circulatory diversion from the left to the right side of the neck through both retia mirabilia following carotid-jugular fistula formation.

A, Schematic diagram, with arrows indicating direction of flow. Main components of the "AVM" are in black. B–D, Frontal left common carotid arteriogram in rapid sequence. *Solid arrows* indicate direction of flow in the common carotid arteries, *arrowhead* indicates both retia mirabilia, and *open arrows* indicate external jugular vein.
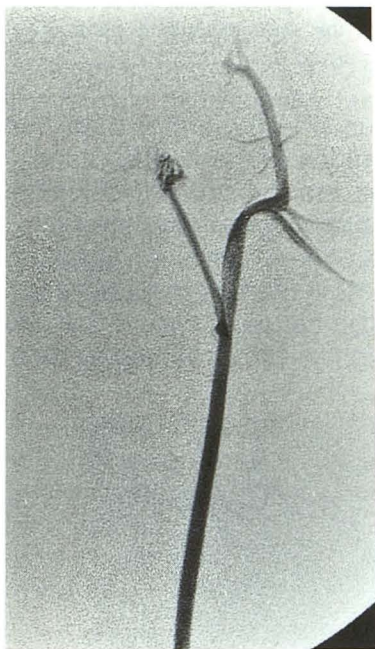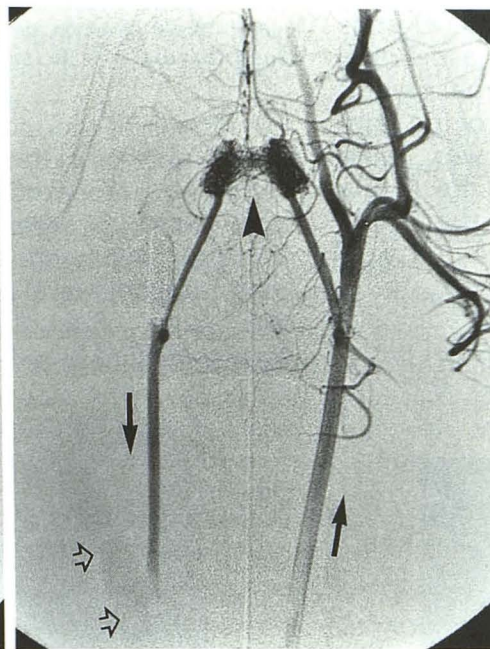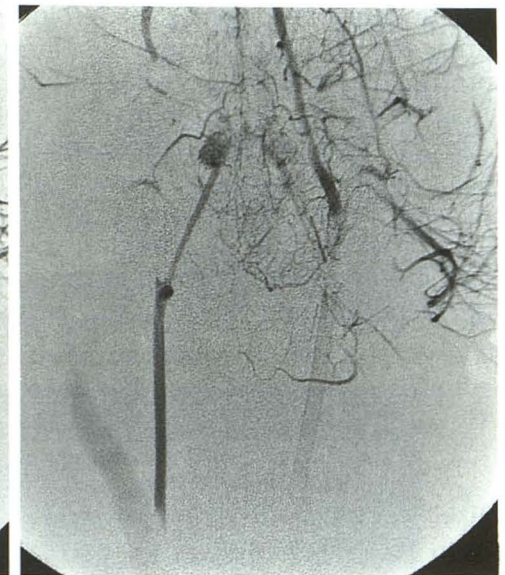
vein drained mostly the face and basal venous sinuses of the head.

AVM Model

Immediate postoperative angiography demonstrated a successful acute-phase simulation of an AVM in all but two swine, in both of which the left ascending pharyngeal artery ("feeder") became occluded because of preoperative catheter-induced trauma. Upon selective injection of the left common carotid artery or ascending pharyngeal artery, a very rapid angiographic sequence was observed in successful models: orthograde flow in the left ascending pharyngeal artery (feeder), shunting through both retia mirabilia across the midline (nidus), and rapid retrograde flow down the right ascending pharyngeal artery and common carotid artery (draining vein) to the fistula (Fig 3). An-
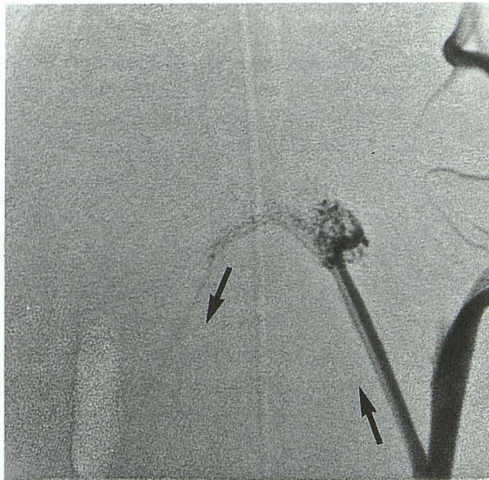
Fig 4. Detail from frontal view of AVM nidus. Preferential retrograde filling of the right ascending pharyngeal artery before the left internal carotid artery. *Straight arrows* indicate direction of flow.

Fig 6. Superselective angiogram via the left middle meningeal artery (*open arrows*) showing the ramus anastomoticus (*short solid arrow*) that supplies the proximal aspect of the AVM nidus. Blood diversion down the right ascending pharyngeal artery toward the fistula (*long arrow*).

giographic steal from the circle of Willis was consistently observed as evidenced by (*a*) preferential retrograde filling of the right ascending pharyngeal artery before the left internal carotid artery (Fig 4), and (*b*) delayed filling of the right internal carotid artery while blood was being diverted down the draining vein to the fistula (Fig 5). Similar blood diversion to the fistula was observed on superselective angiograms of the ramus anastomoticus (Fig 6) and arteria anastomotica (Fig 7). Imaging with craniocaudal tube angulation provided the optimal plane for visualization of shunting across the mi-

crovessels of the nidus (Fig 8). Other than the direct route from the nidus to the fistula (established by preoperative endovascular occlusion or "pruning" of other branches, as outlined previously), there were no other obvious normal or abnormal collateral pathways that resulted from the "sump" effect of the fistula. Beyond the fistula, opacified blood in the external jugular vein
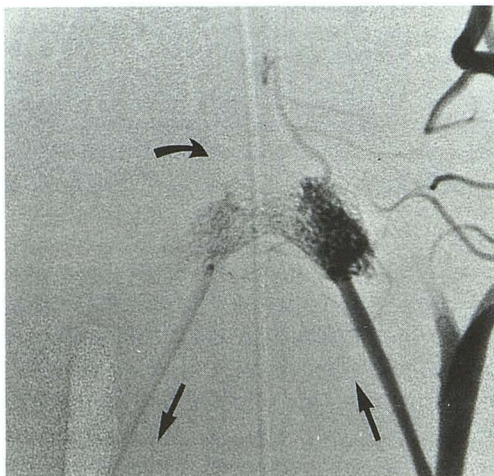

Fig 5. Detail from frontal view of AVM nidus. Delayed filling of the right internal carotid artery (*curved arrow*) with diversion of flow down the right ascending pharyngeal artery. *Straight arrows* indicate direction of flow.
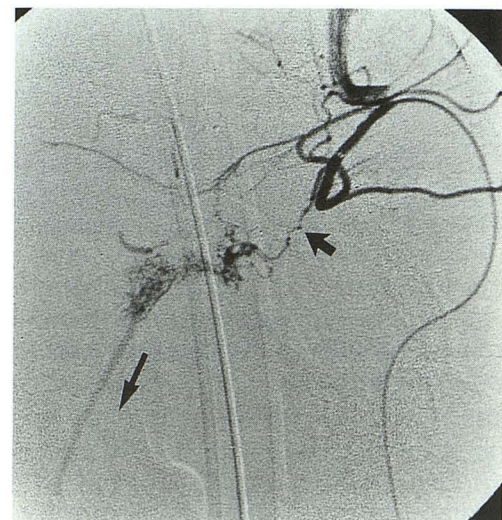

Fig 7. Superselective angiogram with tip of microcatheter at orifice of the arteria anastomotica (*short arrow*). There is filling of the rostral aspect of the AVM nidus. Blood diversion down the right ascending pharyngeal artery toward the fistula (*long arrow*).
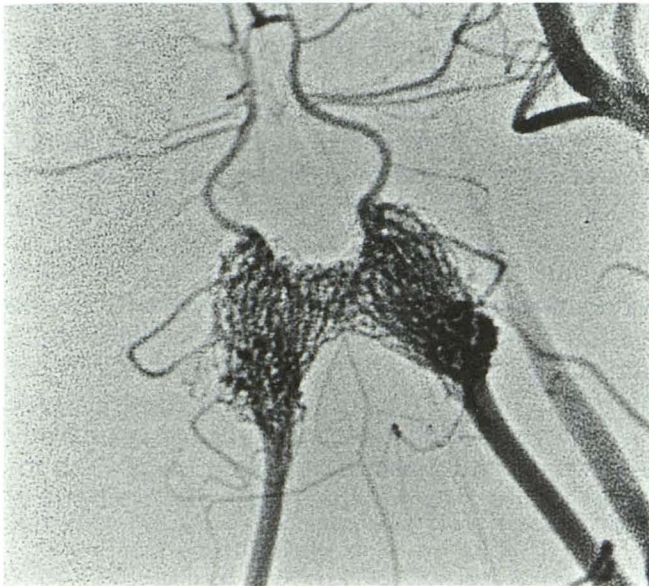
Fig 8. Optimal visualization of nidus microvessels obtained with craniocaudal tube angulation in the frontal plane.

dispersed mostly in an orthograde direction. Retrograde flow was also seen but only reached the region of the lower face.

Discussion

This swine (Sus scrofa) offers several advantages for the purpose of constructing experimental AVM models: (a) it has large neck vessels that can be surgically manipulated with ease during formation of a carotid-jugular fistula; (b) its blood coagulation system is similar to the human, a significant feature when attempting to model a human vascular pathology (14); (c) it is appropriate from an economical and ethical point of view (15); and most importantly (d) it possesses a carotid rete mirabile.

Morphology of the Rete Mirabile

The carotid rete mirabile is a well-developed vascular structure present in some ungulates of the order Artiodactyla, including the swine. Theories of the function of the rete in these animals have been numerous (including its action as a heat-exchange organ or as a regulator of blood pressure to the brain) but mostly inconclusive (16). Before passing through the cartilage of the foramen lacerum, the ascending pharyngeal artery divides into a small number of arterioles. As these pass intracranially, fur-

ther division results in a compact network of microvessels surrounded by the cavernous sinus. Thus, in the swine, there is a minor extracranial and a major intracranial portion to each rete mirabile. Bilateral retia are interconnected by extensions that hug the posterior wall of the sella turcica. At its most rostral end, the rete receives a communication from the external carotid artery through the orbital fissure— the arteria anastomotica. More proximally, the rete receives the ramus anastomoticus from the middle meningeal artery. At the rostral medial end of the plexus is a single vessel, the reconstituted internal carotid artery, which pierces the dura to join the circle of Willis.

The complex plexus of microarteries that make up each rete extensively anastomose to give the appearance of a single structure on gross examination, after removal at autopsy. Bilateral retia and their midline connections measure about $2 \times 1.5 \times 0.2$ cm in size (17). Individual rete vessels can be as large as 700 μm in diameter (16). In one study, however, they ranged in size from 70 μm to 275 μm, with a mean of 154 μm (18). Appropriately, this is comparable to the size of vessels in a human AVM nidus. In one micrometric study of human AVM specimens, the average size of a nidus vessel was 265 μm (19). Histologically, the normal rete vessels are relatively thick-walled compared with the abnormal vascular channels in a human AVM (17). Light microscopy reveals a well-defined undulating internal elastic lamina, and a predominantly muscular tunica media with an average width of 36 μm. Sparse connective tissue is found between vessels.

Carotid-Jugular Fistula

The rete mirabile of swine has a rather similar angiographic appearance to a plexiform nidus of a cerebral AVM (10), but has comparatively low blood flow because of a small drop in intravascular pressure between its afferent and efferent arteries. However, cerebral AVMs possess high shunting flow induced by significant arteriovenous pressure gradients.

Large human (20) and experimental (6–9) arteriovenous fistulas of the neck are often known to have a significant "sump" effect. This phenomenon causes such fistulas to recruit arterial blood at a rapid rate from ipsilateral and contralateral neck vessels. Theoretically, it was thought possible to make use of this effect in an

experimental setting to divert and accelerate flow through both retia of the swine (across the midline) by a distant unilateral carotid-jugular fistula. Moreover, a large surgically-created neck fistula would reduce considerably the chance of spontaneous thrombosis at the source of arteriovenous shunting and establish a large arteriovenous connection away from the rete itself. Both the common carotid artery and external jugular vein are large and easily accessible vessels in the neck of the swine. Surgical creation of a side-to-side fistula using these vessels is simple and can be mastered relatively quickly. The surgery takes approximately 30 to 40 minutes. An added theoretical advantage of a surgical carotid-jugular fistula is that its size (which can be fashioned at will) may provide a means of regulating the degree of sump effect and hence the amount and velocity of shunting across the nidus. This mechanism, however, would require further validation before practical use in future hemodynamic or endovascular therapeutic studies.

AVM Model

In this preliminary study, we have assessed the feasibility of constructing and angiographically demonstrating an in vivo AVM model, with the following characteristics: (a) simplicity of creation; (b) the morphologic components of a human AVM (ie, arterial feeder/s, a nidus, and draining vein/s); (c) arteriovenous shunting through an intact nidus; and (d) steal from the circle of Willis. Angiographic appearances of all successful models were strikingly similar to simple human AVMs. The low intravascular pressure induced by the carotid-jugular fistula always resulted in recruitment of contralateral blood at a fast rate through both retia and reversed the flow in the ipsilateral ascending pharyngeal artery and segment of common carotid artery above the fistula, thus giving the angiographic resemblance of a draining vein. Accordingly, the contralateral ascending pharyngeal artery simulated a terminal arterial feeder, whereas the contralateral ramus anastomoticus and arteria anastomotica simulated en passage feeders to an AVM. The flow down the draining vein was preferential, and resulted in delayed filling (angiographic steal) of the circle of Willis ipsilateral to the fistula.

In human AVMs, there are no normal arteries that exit the nidus to supply cerebral tissue; only veins drain these malformations. Therefore, the presence of both normal internal carotid arteries emerging from the nidus of the AVM accounted for the main angiographic dissimilarity of this model with human AVMs. This feature has to be acknowledged as a morphologic shortfall of the model but one to be weighed against the several significant advantages it offers. Theoretically, to eliminate these normal arteries arising from the nidus and to increase blood diversion to the fistula, it would be desirable to occlude both internal carotid arteries. However, it would not be practicable either to clip surgically (because of their deep skull-base position) or selectively to occlude endovascularly (because of their inaccessibility beyond the retia) one or both of these vessels.

Conclusion

We have demonstrated the feasibility of an AVM model in swine. This model appears to offer several advantages over previously reported models: (a) ease of construction, using principally a standard surgical technique of carotid-jugular fistula formation and simple endovascular occlusive techniques; (b) no iatrogenic injury to the rete mirabile, which constitutes the nidus of the AVM; (c) fast flow through a nidus, with potential to regulate the extent of arteriovenous shunting by surgery; and (d) clear visualization of one main terminal feeder, two en passage feeders, a nidus, and a draining vein. These features should make this an attractive model for testing new embolic materials, training or gaining experience in endovascular therapeutic techniques, and histopathologic verification after embolotherapy.

References

1. Martin N, Vinters H. Pathology and grading of intracranial vascular malformations. In: Barrow DL, ed. *Intracranial Vascular Malformations: Neurosurgical Topics.* American Association of Neurological Surgeons, 1990:1–31
2. Padget DH. The development of the cranial arteries in the human embryo. *Contrib Embryol* 1948;32:205
3. Bartynski WS, O'Reilly GV, Forrest MD. High-flow-rate arteriovenous malformation model for simulated therapeutic embolization. *Radiology* 1988;167:419–421
4. Kerber CW, Flaherty LW. A teaching and research simulator for therapeutic embolization. *AJNR Am J Neuroradiol* 1980;1: 167–169
5. Hecht ST, Horton JA, Kerber CW. Hemodynamics of the central nervous system arteriovenous malformation nidus during particulate embolization: a computer model. *Neuroradiology* 1991;33: 62–64

6. Bederson JB, Wiestler OD, Brüstle O, et al. Intracranial venous hypertension and the effects of venous outflow obstruction in a rat model of arteriovenous fistula. *Neurosurgery* 1991;29:341–350

7. Morgan MK, Anderson RE, Sundt TM. A model of the pathophysiology of cerebral arteriovenous malformations by a carotid-jugular fistula in the rat. *Brain Res* 1989;496:241–250

8. Spetzler RF, Wilson CB, Weinstein P, et al. Normal perfusion pressure breakthrough theory. *Clin Neurosurg* 1978;25:651–672

9. Scott BB, McGillicuddy JE, Seger JF, et al. Vascular dynamics of an experimental cerebral arteriovenous shunt in the primate. *Surg Neurol* 1978;10:34–38

10. Lylyk P, Viñuela F, Vinters HV, et al. Use of a new mixture for embolization of intracranial vascular malformations: preliminary experimental experience. *Neuroradiology* 1990;32:304–310

11. Chaloupka JC, Viñuela F, Duckwiler GR. Creation of a true arteriovenous malformation in swine: a preliminary feasibility and natural history study. In: Proceedings of the 78th scientific assembly and annual meeting of the Radiological Society of North America; 1992; Chicago

12. Stehbens WE. Blood vessel changes in chronic experimental arteriovenous fistulas. *Surg Gynecol Obstet* 1968;127:327

13. Beck CS, McKhann CF, Belnap WD. Revascularization of the brain through establishment of a cervical arteriovenous fistula. *J Pediatr* 1949;35:317–329

14. Osterman FA, Bell WR, Montali RJ, et al. Natural history of autologous blood clot embolization in swine. *Invest Radiol* 1976;11:267–276

15. Orlin JR, Osen KK, Hovig T. Subdural compartment in pig: a morphologic study with blood and horseradish peroxidase infused subdurally. *Anat Rec* 1991;230:22–37

16. Dieguez G, Garcia AL, Conde MV, et al. In vitro studies of the carotid rete mirabile of Artiodactyla. *Cardiovasc Res* 1987;33:143–154

17. Brothers MF, Kaufmann JCE, Fox AJ, et al. N-butyl-cyanoacrylate: substitute for IBCA in interventional neuroradiology: histopathologic and polymerization time studies. *AJNR Am J Neuroradiol* 1989;10:777–786

18. Lee Dh, Wriedt CH, Kaufmann JCE. Evaluation of three embolic agents in the pig rete. *AJNR Am J Neuroradiol* 1989;10:773

19. Isoda K, Fukuda H, Takamura N, et al. Arteriovenous malformation of the brain: histological study and micrometric measurement of abnormal vessels. *Acta Pathol Jpn* 1981;31:883–893

20. Halbach VV, Higashida RT, Hieshima GB. Treatment of vertebral arteriovenous fistulas. *AJNR Am J Neuroradiol* 1987;8:1121–1128

21. Daniel PM, Dawes JDK, Prichard MM. Studies of the carotid rete and its associated arteries. *Philos Trans R Soc London* 1953;237:(series B)173–208